

6102449

MAGNETOTELLURIC SURVEY

in the

SODA LAKE AREA

of

NEVADA

for

CHEVRON RESOURCES

GEOTRONICS CORPORATION

10317 McKalla Place

Austin, Texas 78758

Darrell R. Word, Chief Scientist

David Halpin, Senior Geophysicist

Ken Owens, Geologist

Report No.

TABLE OF CONTENTS

<u>Section</u>	<u>Page No.</u>
I. Introduction	I-1
II. Data Displays and Discussion of Results	II-1
A. Introduction	II-1
B. Data Displays	II-1
1. Site Location Map	II-1
2. Resistivity Cross Section Based on One-Dimensional Inversions; Dip-Axis Directions	II-1
3. Correlation Cross Section Based on One-Dimensional Inversion	II-3
4. Three Dimensionality Indices	II-5
5. Anisotropy Factor and Anisotropy Sense Cross Sections	II-6
C. Discussion of Results	II-7
1. Resistivity Cross Section Based on One-Dimensional Inversions; Dip-Axis Directions	II-7
2. Correlation Cross Section Based on One-Dimensional Inversions	II-9
3. Three Dimensionality Indices	II-9
4. Anisotropy Factor and Anisotropy Sense Cross Sections	II-9
III. Conclusions and Recommendations	III-1
A. Conclusions	III-1
B. Recommendations	III-3

Selected Bibliography

APPENDICES

Appendix A - Field Operations

Appendix B - Data Processing Procedure

Appendix C - MT Analysis -- Defining Equations and Glossary of
Computed Quantities

Appendix D - MT Interpretation -- Defining Equations and Glossary
of Computed Quantities

Appendix E - Resolution

Appendix F - Data Smoothing and Comments on Noise and Special
Conditions

LIST OF PLATES

- | | |
|-----------|---|
| Plate 1.1 | Site Location Map |
| Plate 2.1 | Resistivity Cross Section Based on One-Dimensional Inversions; Dip-Axis Direction |
| Plate 3.1 | Correlation Cross Section Based on One-Dimensional Inversions |
| Plate 4.1 | Three-Dimensionality Indices - Tensor Impedance, Skew and Ellipticity |
| Plate 5.1 | Anisotropy Factor and Anisotropy Sense Cross Section |

I. Introduction

In late March, 1977 Geotronics Corporation conducted a Magneto-telluric Survey near Soda Lake, Nevada for Chevron Resources Company. The magneto-telluric data were to be utilized to further delineate the subsurface resistivity structures seen on a previous survey performed in 1975. Data were acquired employing a Geotronics Corporation MT system utilizing field digital recording. A full five component electromagnetic field measurement was made at each site in the frequency range 0.002 Hz to 250 Hz, and the complete tensor MT analysis was used. Data were processed in Austin, Texas with computer processing utilizing the Houston Based CDC 6600 with a remote terminal. Various displays of the MT results were produced for presentation in this report. The MT results at various sites were subsequently correlated and interpreted. Discussions of these correlations are included, followed by a series of conclusions and recommendations based upon the results. Also included in this report are Appendices A through F, which present additional information on field operations, data processing and modeling procedures, the mathematical definitions of the Magnetotelluric parameters, and an assessment of the data quality. For more detail concerning these items the reader is referred to Word, et al, (1970) and other literature.

Data quality throughout the area ranged from fair to poor. Data at sites 2 and 3 were poor whereas data at sites 1 and 4 were fair below 0.5 Hz and .1Hz, respectively.

II. Data Displays and Discussion

A. Introduction

For this report Geotronics Corporation has prepared a series of displays containing parameters derived from the magnetotelluric data. These displays are composite presentations of single site information and provide the basis for establishing correlations along the traverses. Each display presents a different parameter, or a different aspect of a parameter, and provides input towards the final interpretation. The displays will be described first followed by a discussion of the results obtained from the survey.

B. Data Displays

1. Site Location Map

The site map (Plate 1) shows MT site locations on a topographic base map. Section lines are illustrated, along which the vertical cross section information is displayed on the following plates. All vertical cross sections are scaled to the site map.

2. Resistivity Cross Section Based on One-Dimensional Inversions; Dip-Axis Directions

Plate 2.1 displays an interpreted true resistivity structure. For each site, a one-dimensional model inversion was done for the

RTE (f) apparent resistivity-frequency function (E parallel to strike), to produce a resistivity-depth function $R(z)$. An adaption of the Bostick inversion method (see Appendix D) was used to produce $R(z)$ as a continuous function, employing the "amplitude inversion" mode in all cases. In Plate 2.1 the vertical cross section is constructed as a composite of the $R(z)$ functions. Resistivity values are tabulated at discrete points on the depth scale and contoured on constant resistivity.

The models presented in Plate 2.1 and all MT models derived as a composite of the 1D model inversions should be viewed as estimates of the volume averaged or smoothed electrical structures, where the dimensions of the averaging volume are approximately proportional to depth. The depth coordinate in the models represents mean depth of the averaging volume. The resistivity and dip-axis angle values result from the net influence of the structure within the averaging volume. This averaging concept is not mathematically precise but offers a reasonable intuitive view of the smoothing influence.

Dip-Axis directions versus depth are shown in plan view above the resistivity section. The dip-axis direction is given by the angle $A(YZ)$ (See Appendix C) determined from the vertical magnetic field. The dip-axis represents the direction of maximum gradient in the electrical structure, with 180 degree ambiguity

(i. e. the polarity of the gradient is not given by this quantity), and is a line normal to the apparent strike vs. frequency. Dip-axis information is displayed at each site location on a polar plot with a radial logarithmic depth scale. The computed frequency-domain functions are plotted on the depth scale via a pseudo depth-frequency relationship $z(f)$ produced by the RTE inversion process (there is no precise one-to-one depth-frequency correspondence). The unsmoothed $A(YZ)$ data points and the 180 degree complements are plotted so that directional trends may be deduced from patterns in the scattered data. The degree of scatter in the dip-axis data depends on the degree of directional preference caused by the electrical structure. Tighter grouping indicates a stronger directional trend, whereas the scatter approaches 360 degrees for data where the degree of directional preference is small.

3. Correlation Cross Section Based on One Dimensional Inversions

Plate 3.1 displays the correlation section with the same information shown on both logarithmic and linear depth scales. This display is derived by first plotting the continuous 1-D resistivity inversion $R(z)$ data for each site on a resistivity-depth scale at each corresponding site location (similar to a bore-hole log correlation display). The $R(z)$ curves for both the "amplitude inversion" mode

(solid curve) and the "phase inversion" mode (dotted curve) are plotted in the display. The "amplitude inversion" mode of $R(z)$ is used in the correlation process. A layered sequence is interpreted at each site by assuming interfaces at the inflection points in the $R(z)$ function. Correlation lines through the inflection points are drawn from site to site, connecting associated features and signatures of the $R(z)$ functions along the traverse. In this manner, even small features that are close to the noise level of the sounding may be interpreted when site to site correlation can establish sufficient credibility.

It is noteworthy that the process up to the act of correlating sequences along the traverse is a precisely defined, purely analytical procedure, and the results are stable and unique for each measuring site within noise limitations. The correlation process, however, is more subjective and a solution is not necessarily unique. The correlation process is done with learned discretion by the interpreter and is constrained by other known geological and geophysical information, and by the requirement of compatibility with the total observed MT response, including anisotropic effects.

The process used recognizes relatively resistive or conductive units between inflection points of $R(z)$. The absolute value of resistivity is also considered in the correlation process;

but due to the smoothing effect in the MT response, the $R(z)$ value for a given structure is affected by the relative thickness of the structure as well as its intrinsic resistivity. It is also true that the intrinsic resistivity of a given rock type can change from one point to another with a change in the local conditions. The resistivity is therefore not expected to necessarily remain constant along a correlated unit.

The logarithmic depth scale is used to facilitate the correlation process and to display the results on a constant resolution scale. Since the minimum dimensions of a detectable unit are approximately proportional to its depth, a given size plot feature in one place on the scale is of comparable resolution to a feature of the same size in another place on the scale.

The correlation results are also presented on a linear depth scale to facilitate the physical interpretation.

4. Three Dimensionality Indices

Plate 4 displays the skew and ellipticity (ALPHA and BETA in Appendix C) of the tensor impedance, both of which range in magnitude from 0 to 1.0 and indicate the degree of three dimensionality present in the MT response. ALPHA = 0 and BETA = 0 are necessary and sufficient conditions for two dimensionality (including one dimensionality). Two dimensionality in the MT response means that

the electrical structure is symmetrical about some vertical plane that passes through the measuring site (including a two-dimensional structure). The dip-axis would lie in that vertical plane of symmetry. A non-zero value for ALPHA or BETA indicates three dimensionality, meaning there is not vertical plane of symmetry for the structure. In such case, the dip-axis still defines the axis of maximum change. Certain qualitative aspects of the structure can be deduced from the nature of the 3D indices, as discussed briefly in Appendix B and more fully in Word, et (1970).

In the display, the unsmoothed estimates of ALPHA and BETA are shown in a vertical section with logarithmic depth plots superimposed at each corresponding site location. The frequency domain 3-D indices are related to depth via the pseudo-frequency relationship $z(f)$ produced by the RTE inversion process.

5. Anisotropy Factor and Anisotropy Sense Cross Section

Plates 5.1 displays the anisotropy factor and anisotropy sense values (AF and AS in Appendix D) contoured on vertical cross sections. The frequency domain functions are referred to the depth scale via the pseudo depth-frequency relationship $z(f)$ from the RTE inversion.

The anisotropy factor, $AF = RTM/RTE$, is an indicator of lateral change in the structure. $AF = 1$ for a one-dimensional structure, and $AF \neq 1$ where lateral inhomogeneity (apparent anisotropy) exists.

As the MT sounding depth increases, AF changes only through depth ranges where a laterally anomalous horizon is encountered, and it remains otherwise constant at the value imparted by any shallower anomalies. A change in AF along a traverse line indicates a change in the structure at or above the level for which the change in AF is observed. Abrupt lateral changes, such as near surface vertical contacts, are characterized by steep or near vertical contours in AF.

The anisotropy sense (AS) is based on the change in AF with frequency (or depth). By the convention used herein, $AS = 0$ indicates one dimensionality, $AS > 0$ indicates a dominant resistive anomaly, and $AS < 0$ indicates a dominant conductive anomaly, for the frequency or depth range that is effective.

(A study and further development of the anisotropy factor and sense parameters is one of the current Geotronics R & D efforts. Because of some obvious features of interest, the AF and AS results are presented here as an experimental display, but without exhaustive treatment in this report).

C. Discussion of Results

1. Resistivity Cross Section Based on One-Dimensional Inversions; Dip-Axis Directions (Plate 2.1)

Plate 2.1 illustrates the contoured Resistivity Cross Section based on One-Dimensional Inversions for the four sites recorded in March 1977. (For reference, Site 1-3 of the original 1975 survey

would lie halfway between sites 1 and 2 of this cross section). The section is characterized, in general, by zones of low resistivity materials. Near surface resistive zones are present at sites 4, 3 and 1. A shallow conductive zone, on the order of 1-3 ohm-meters is pervasive at +2200 to +2800 feet. Below this, a thick zone of varying resistivity is present. This zone varies from about 6000 feet to 14,000 feet thick. Resistivities within the zone vary from 5 to 14 ohm meters. The higher resistivities are present in the northern portion of the line where the zone appears to be thickest. Immediately beneath this broad zone is the "deep" conductor. Resistivities range from 0.2 to 1.6 ohm meters. The surface described by this zone appears to shallow from -29,000 feet beneath site 1 to -8000 feet beneath site 3. At depth, below site 1 (-34,000 feet), and site 2 (-26,000 feet), the section again starts to become slightly more resistive.

The new data fits well with the original survey data. If site 1-3 of the original survey were plotted, only minor contour adjustment would be needed. That information would cause a shallowing of the deeper conductive contours between sites 1 and 2.

Dip-axis data are consistent along the traverse. These data show a N-S to N20E strike direction. Data from sites 3 and 4 are quite tight. Data at site 1 are moderately scattered and data at site 2 are very scattered.

2. Correlation Cross Section Based on One-Dimensional Inversions

Plate 3.1 illustrates the correlation base on one-dimensional inversions. Correlations across the area are consistent with the resistor-conductor sequence readily trackable. Noteable are (1) the near surface resistive "kick", (2) the pervasive shallow conductor which exhibits minor resistive kicks, (3) the thick "resistive" zone, and (4) the "deep" conductor.

Trends in the correlation data indicate an apparent deepening to the northeast.

3. Three-Dimensionality Indices

Tensor impedance skew and ellipticity data are presented on Plate 4.1. The data indicate that beneath sites 4 and 2 uncoupled anomalies exist below 8000 feet and 10,000 feet respectively. This type of anomaly indicates the coincidence of two or more anomalies in different directions from the site (as opposed to seeing one anomaly through another). Beneath site 1 uncoupled anomalies exist from 0 - 1200 feet, 4500 - 10,000 feet and from 13,000 - 30,000 feet. Data at site 3 indicate high levels of both skew and ellipticity, indicating high three dimensionality, from 8000 to 12,000 feet beneath the site.

4. Anisotropy Factor and Anisotropy Sense Cross Sections

Plate 5.1 illustrates the anisotropy factor and anisotropy

sense information. The anisotropy factor data indicate that moderate to high levels of anisotropy exist. Lowest anisotropy is exhibited beneath site 1. Beneath sites 2 and 4 anisotropies range from 3-4. High anisotropy exists at shallow levels beneath site 3. Anisotropy values of 10 are present at +1500 feet.

The anisotropy sense section depicts a general conductive nature to the Section. A strong conductive anomaly is indicated at -9000 feet beneath site 3. Scattered resistive anomalies are indicated at various levels beneath sites 4, 2 and 1.

III. Conclusions and Recommendations

A. Conclusions

As a result of the additional magneto-telluric sites in the Soda Lake area the following can be concluded:

(1) The shallow conductive zone, called the Lower Lahontan Valley Group in the earlier report, persists to the Southwest. The more conductive portion, less than 2 ohm meters, exists beneath sites 2, 3 and 4 of this survey and beneath sites 1-1 through 1-5 and sites 1-7 through 1-9 of the original survey. Therefore a northern and eastern limit can be established for this less than 2 ohm-meter zone.

(2) The second zone down, that referred to as Tertiary rhyolites and volcanics in the original report, exhibits resistive

and conductive trends. The more resistive portion of the zone lies beneath sites 1 and 4 and beneath sites 1-3, 1-4, and 1-5 through 1-10. The conductive portion lies beneath sites 2 and 3 beneath sites 1-1 and 1-2. Thus, a northeasterly trend for the conductive portion is established by the sites. This conductive trend appears to pass through Soda Lake. This conductive trend may represent intensely altered rhyolites and volcanics in the Trukee Formation (?) of the original report and/or a fracture zone. Lineations of contours to the northeast of the survey area have the same orientation.

(3) The "deep" conductive zone, referred to as the magma chamber in the original report, shallows from the north to the vicinity of site 3 and from west to east. Lowest resistivities at or near this interface exist beneath sites 3 and 4 and beneath sites 1-1, 1-2 and 1-5. Beneath sites 1 and 2, and perhaps site 4, the resistivities appear to begin rising again, possibly indicating a "bottom". Thus, the data begin to define a shape and trend to this important conductive anomaly. The dominant trend is northeasterly through sites 3, 4 and 1-1 and 1-2. To the north the conductor may have a bottom implying the existence of an arm.

(4) The magneto-telluric method appears well suited for tracking anomalies in the Soda Lake area.

B. Recommendations

As a result of this survey we would recommend the following:

(1) If interest is in the shallow conductor, additional sites should be placed to the west to define its western limits;

(2) If interest is in the conductive portion of the Tertiary rhyolite and volcanic section, sites should be placed to the west and east of Soda Lake, and

(3) If interest is in further delineation of the deep conductor, with the assumptions that (a) the "arm" is real and (b) resistivity value is related to temperature gradient, then additional sites should be established. Location of these sites would have to be to the west and east of Soda Lake. Additional sites in the vicinity of site 1-5 would be needed to solve the question of why it is so conductive and "off-trend". Attempts at all sites should be made to record long enough to penetrate the "arm" of the conductor as at several sites it appears that the conductor was penetrated. As sites are located closer to the conductive "core" of the anomaly, longer recording time would be needed to penetrate the conductive "arm".

Appendix A - Field Operation

Five orthogonal component, surface EM field measurements (E_x , E_y , H_x , H_y , H_z) are made of the micropulsation fields at each site in the overall frequency range of approximately 0.002 to 250 Hz. This range was covered by five overlapping bands as described in Table B-1.

Figure A-1 shows the field sensor configuration used. The positive x-axis is directed to magnetic north, in a right-hand coordinate system. The E-field sensors are electrode lines using Cd-CdCl₂ or Pb electrodes with a usual spacing of 300 feet. The H-field sensors are Geotronics induction magnetometers - Model MTC-4SS for H_x and H_y , and Model MTC - 6SS for H_z . A vertical axis air core loop is also available for H_z where needed.

The instrument van contains the recording system of Geotronics manufacture, consisting of the MTE-4 three-channel E-field preamplifier, the MTH-4 three-channel H-field preamplifier, the MTC-2 calibrator, the MTF-16 filter-post amplifier, and the MTDR-2 digital recorder. A six-channel Brush chart recorder is used for field monitoring of the signals.

A five-man crew is used, consisting of the crew chief and instrument man, alternate instrument man, and a three-man site layout team including a surveyor.

Proper field technique, which is of extreme importance in MT recording, has been developed by Geotronics personnel through 16 years of MT experience and is stressed throughout the survey. System noise and data quality checks are made routinely. All sensors are buried about 12 inches or more deep and all cables buried or weighted to reduce wind noise and improve thermal stability. While one site is

being recorded, an alternate set of sensors is installed at the next site, and an adequate time (a few hours) is allowed for stabilization, including thermal and magnetic stabilization of the magnetometers and contact potential stabilization of the electrodes.

Field tapes are sent back to Geotronics daily (when conditions permit) so that preliminary analysis can be done to assess signal quality while the field crew is still in the survey area.

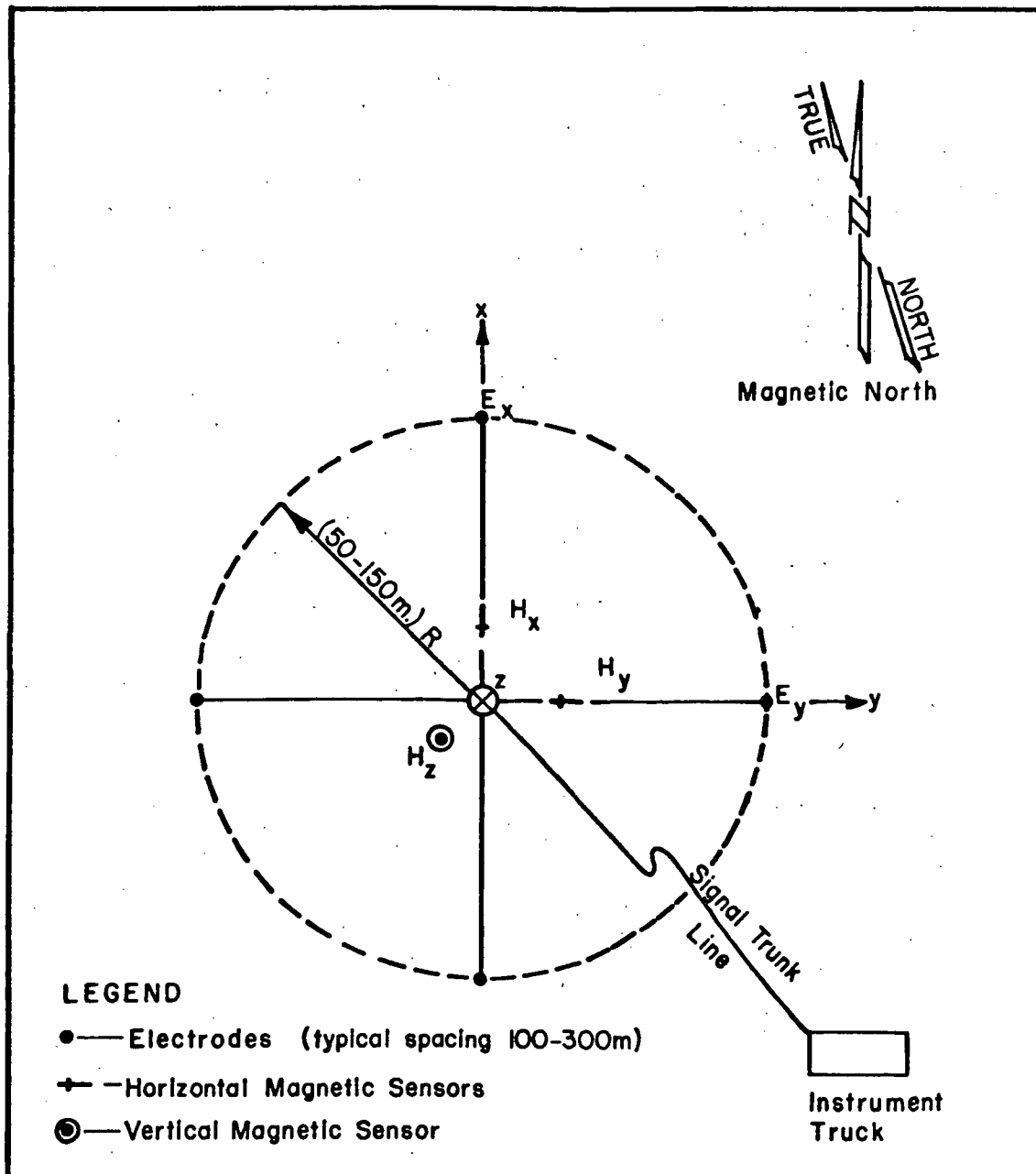


Fig. A-1: Magnetotelluric Field Sensor Layout.

PROPRIETARY INFORMATION NOTICE
 This document contains Geotronics Corporation proprietary and confidential information which is supplied for limited purposes only, and remains the property of Geotronics Corporation. This document may not be reproduced in whole or in part without written consent of Geotronics Corporation and the information therein must not be disclosed to persons not having need of such disclosure consistent with the License for which it is supplied. This document is to be returned to Geotronics Corporation upon termination of the License under which it is supplied.

Appendix B - Data Processing Procedure

The MT data processing, from field data through the final interpretation, is divided into two phases; (1) analysis and (2) interpretation. Mathematical definitions for the two phases are outlined in Appendices C and D respectively.

The field data represents a measurement of the total vector E and H fields (electric and magnetic fields respectively) on the surface at the measuring site. The basic output of phase (1) is a set of tensor quantities that totally and uniquely express the surface E and H field interrelationship at the point of the measuring site. With $[\bar{E}]$ and $[\bar{H}]$ representing horizontal vector fields (there is no vertical E at the surface), the basic field relationships can be expressed by the frequency domain matrix equations,

$$[\bar{E}] = [Z] [\bar{H}] \quad (B-1)$$

$$\text{and } [H_z] = [k_z] [\bar{H}] \quad (B-2)$$

where the tensors $[Z]$ (surface impedance) and $[k_z]$ are, within noise limitations, a function of only the subsurface electrical structure, and they contain all of the MT information available at the site. The same information is, however, expressed in other forms (see Appendix C) for convenience. The analysis results are obtained for all measuring sites, which should represent a spatial sampling of the structure being investigated.

The phase (2) objective is to interpret the set of $[Z]$ and $[k_z]$ functions for all sites (as sampled functions of frequency and space on the surface) in terms of the subsurface structure. The interpretation phase is essentially an open ended problem because of limitations

due to noise, finite sampling of the data, and lack of precise analytical solutions for 3-D geometry. The interpretation must be done by approximate modeling solutions and must deal with a certain degree of non-uniqueness imposed by the limitations mentioned. The non-uniqueness, which occurs in varying degrees depending on the problem, gives rise to the fact that the best interpretation is obtained by use of all available geological and geophysical information to constrain the process. Ideally, the approach is to choose the overlap or domain of compatibility between sets of acceptable models for the MT and other data, thereby reducing the number of possible models. In practice non-uniqueness does not uniformly affect all aspects of the model, which usually has some aspects that are well determined and some that are not. The 1-D resistivity-depth profile, for example, normally has a faithful stratigraphic sequence, while the depth and/or true resistivity of a given unit may be uncertain to some degree.

The standard modeling procedure (See Appendix D) produces for each site an estimate of the (1) continuous, one-dimensional, true resistivity-depth function $R(z)$ and a pseudo depth-frequency correspondence, $z(f)$, (2) the dip-axis direction $A(YZ)$ as a function of depth, z , (3) the anisotropy indices AF and AS as a function of depth, and (4) the 3-D indices, $ALPHA$ and $BETA$ as a function of depth. Assemblages of the one-dimensional functions are produced to represent the volume averaged or smoothed 3-D electrical structure. More complicated models are then applied to refine portions of the first model if justified by need and economics for a given case.

Finally, the geological interpretation is done, if requested, using all MT information and other control information available.

Computer processing is done on the Control Data Corporation Cybernet System. The Houston based CDC6600 is used and accessed.

through the CDC-Austin user terminal. Field tapes are sent to Houston and stored in the CDC tape library in read-only mode for the duration of the survey and analysis.

The frequency bands used in the analysis are given in Table B-1, which includes the sampling parameters and the frequency range of results used for each band. The upper limit on the frequency range used is near the alias filter cut-off frequency, which is set to approximately half the Nyquist frequency. The lower three frequency points of the analysis results are omitted to avoid truncation aliasing error that is apt to be present. The analysis frequency bands overlap for redundancy.

Strip chart records and field logs are checked to select the best data recording runs for analysis. Initially, one run of each band for each site is processed and the results checked for several acceptance criteria. Additional runs are processed where needed to produce the best definition of the computed functions. Finally, all runs of the frequency domain results to be used are plotted for use in the subsequent interpretation. Averaged and smoothed functions are produced from the raw results for use in modeling and other interpretation. All data is corrected for local magnetic declination so that all subsequent results can be presented in geographic coordinates.

Table B-1 - Recording Frequency Bands

Band	Post Filter (Hz)	Sampling Rate (Hz)	Number Samples	Frequency Range Used (Hz)	No. Runs Recorded (Nominal)
B6	10-256	1000	4096	2.08-256	4
B5	1-25	100	4096	0.208-25.6	4
B4	0.1-5	20	4096	0.0415-5.12	4
B3	0.01-0.5	2	4096	0.00415-0.512	1-2
B2	0.002-0.125	.5	2048	0.00208-0.128	1

Appendix C

MT Analysis -- Defining Equations and Glossary of Computed Quantities

I. MT Model and Basic Relationships

The total electric and magnetic fields \mathbf{E} and \mathbf{H} in the frequency (f) domain at point '0' on the earth surface are related by

$$\overline{[\mathbf{E}]} = [\mathbf{Z}] \overline{[\mathbf{H}]} \quad (\text{C-1})$$

$$\text{and } [\mathbf{H}_z] = [\mathbf{k}_z] \overline{[\mathbf{H}]} \quad (\text{C-2})$$

$$\text{or } [\mathbf{H}_z] = [\mathbf{Y}_z] \overline{[\mathbf{E}]} \quad (\text{C-3})$$

(excluding $f = 0$), and where

- (1) $\overline{[\mathbf{E}]}$, $\overline{[\mathbf{H}]}$, and $[\mathbf{H}_z]$ are column vectors representing the horizontal \mathbf{E} and \mathbf{H} field components (with bar) and the vertical \mathbf{H} field ($E_z = 0$, due to surface boundary conditions),
- (2) $[\mathbf{Z}]$ is a dyadic tensor representing the surface impedance, relating the horizontal \mathbf{E} and \mathbf{H} fields, and
- (3) $[\mathbf{k}_z]$, $[\mathbf{Y}_z]$ are tensors relating \mathbf{H}_z to the horizontal \mathbf{E} and \mathbf{H} fields, respectively.

$[\mathbf{Z}]$ and $[\mathbf{k}_z]$ or $[\mathbf{Y}_z]$ represent all information present in the MT response for a given site. For an essentially plane wave source, they are functions only of frequency and the earth parameters.

Coordinate System (See Fig. C-1) --

The coordinate system is a standard right hand rectangular (x, y, z - axes) with $+z$ -down (vertical axis) with the origin at point

'0'. The x-axis is rotated clockwise (looking in +z direction) by an angle 'A' from the reference axes xr and yr (normally north and east, respectively). In the rotated coordinate system, all fields and computed tensor quantities are functions of the rotation angle 'A'.

Model --

$z \geq 0$ - semi-infinite conductive half space (solid earth) with a generally 3-D distribution of properties

$z < 0$ - free space

Field Source --

EM plane wave propagating in +z direction (down) and incident on $z = 0$ surface. Any polarization is allowable except at least some degree of random polarization is required by the computation process.

Field Relations in Rectangular Coordinate System --

For the (x, y, z - axes) Equation (C-1), (C-2) and (C-3) become

$$E_x(A) = Z_{xx}(A) H_x(A) + Z_{xy}(A) H_y(A) \quad (C-4)$$

$$E_y(A) = Z_{yx}(A) H_x(A) + Z_{yy}(A) H_y(A) \quad (C-5)$$

$$H_z(A) = k_{zx}(A) H_x(A) + k_{zy}(A) H_y(A) \quad (C-6)$$

$$H_z(A) = Y_{zx}(A) E_x(A) + Y_{zy}(A) E_y(A) \quad (C-7)$$

Equations (C-6) and (C-7) are alternate expressions of H_z (e.g., k_{zx} and k_{zy} can be obtained by substituting (C-4) and (C-5) into (C-7).

Units Used - (MKS) --

E - mv/km

H - gamma *not MKS!*

f - Hz

A - degrees

II. Rotated Quantities

$$\text{Define: } Z1 = Z_{xy} - Z_{yx} \quad (\text{C-8})$$

$$Z2 = Z_{xx} + Z_{yy} \quad (\text{C-9})$$

$$Z3 = Z_{xy} + Z_{yx} \quad (\text{C-10})$$

$$Z4 = Z_{xx} - Z_{yy} \quad (\text{C-11})$$

A. Special values of the rotation angle 'A' for the principal axes of the tensor functions defined in Section I --

$$A(\text{ZMX}): |Z3(A(\text{ZMX}))| = |Z3(A)|_{\text{mx}} \quad (\text{C-12})$$

$$A(\text{KZ}): |k_{zx}(A(\text{KZ}))| = |k_{zx}(A)|_{\text{mx}} \quad (\text{C-13})$$

$$A(\text{YZ}): |Y_{zy}(A(\text{YZ}))| = |Y_{zy}(A)|_{\text{mx}} \quad (\text{C-14})$$

$$A(Z) = \begin{cases} A(\text{ZMX}), (A(\text{YZ}) - 45^\circ) \leq A(\text{ZMX}) \leq (A(\text{YZ}) + 45^\circ) \\ A(\text{ZMX}) \pm 90^\circ, \text{ otherwise} \end{cases} \quad (\text{C-15})$$

B. Rotated tensor components for principal axes.

$$ZTE = Z_{yx}(A(Z)) = |ZTE| / \underline{\text{PTE}} \quad (\text{C-16})$$

$$ZTM = Z_{xy}(A(Z)) = |ZTM| / \underline{\text{PTM}} \quad (\text{C-17})$$

$$\text{RTE} = (0.2/f) |ZTE|^2 \text{ (ohm-meters)} \quad (\text{C-18})$$

$$\text{RTM} = (0.2/f) |ZTM|^2 \text{ (ohm-meters)} \quad (\text{C-19})$$

$$\text{KZTE} = k_{zx}(A(\text{KZ})), (H_z / H \perp \text{ strike}) \quad (\text{C-20})$$

C. 3-D indices (skew and ellipticity)

$$\text{ALPHA} = |Z2/Z1|, \text{ (invariant with 'A')} \quad (\text{C-21})$$

$$\text{BETA} = |Z4(A(\text{ZMX})) / Z3(A(\text{ZMX}))| \quad (\text{C-22})$$

III. Notes and Glossary of Terms

A. Notes

1) Principal values of the rotation angle 'A' for a given tensor function are indicated by a parenthetical suffix on A.

2) A "TE" or "TM" suffix is used on some variable names to indicate transverse electric (E parallel to strike) or transverse magnetic (H parallel to strike) components.

3) Refer to sections I and II for mathematical definitions of the terms described herein.

B. Glossary

1) Dip axis -- a straight line in the $z = 0$ plane, passing through the measuring point and normal to the apparent strike direction; axis of maximum change.

2) A(ZMX) -- principal rotation angle for the $[Z]$ tensor, placing the x-axis in the maximum impedance direction.

3) A(KZ) -- principal rotation angle for the $[k_z]$ tensor, such that H_z is most coherent with H_x ; x-axis is an estimate of the dip-axis.

4) A(YZ) -- principal rotation angle for the $[Y_z]$ tensor, such the H_z is most coherent with E_y ; x-axis is an estimate of the dip-axis.

5) A(Z) -- principal rotation angle for the $[Z]$ tensor, but adjusted by $\pm 90^\circ$ such that the x-axis angle is nearer A(YZ), the dip-axis angle; direction of the TM component of the electric field.

6) ZTE -- principal component of rotated $[Z]$ tensor, for E parallel to strike and H perpendicular to strike.

7) ZTM -- principal component of rotated $[Z]$ tensor, for E perpendicular to strike and H parallel to strike.

- 8) RTE -- apparent resistivity for ZTE
- 9) RTM -- apparent resistivity for ZTM
- 10) PTE -- phase of ZTE
- 11) PTM -- phase of ZTM
- 12) KZTE -- principal component of rotated $[k_z]$ tensor for x-axis aligned with dip-axis (equal to $H_z/H \perp$ strike).
- 13) ALPHA -- skew of $[Z]$ tensor; ratio of magnitudes of phasor positions of the centers of the elliptical loci with rotation angle 'A' for Z_{xx} (numerator) and Z_{xy} (denominator); non-zero value indicates three-dimensionality.
- 14) BETA -- ellipticity of $[Z]$ tensor; ratio of minor to major axes of rotation angle loci ellipse; non-zero value indicates three-dimensionality.

IV. Reference

Word, D. R., H. W. Smith, F. X. Bostick, Jr., "An Investigation of the Magnetotelluric Tensor Impedance Method," Electrical Geophysics Research Lab., Tech. Report No. 82, Univ. of Texas, Austin, Texas, 1970.

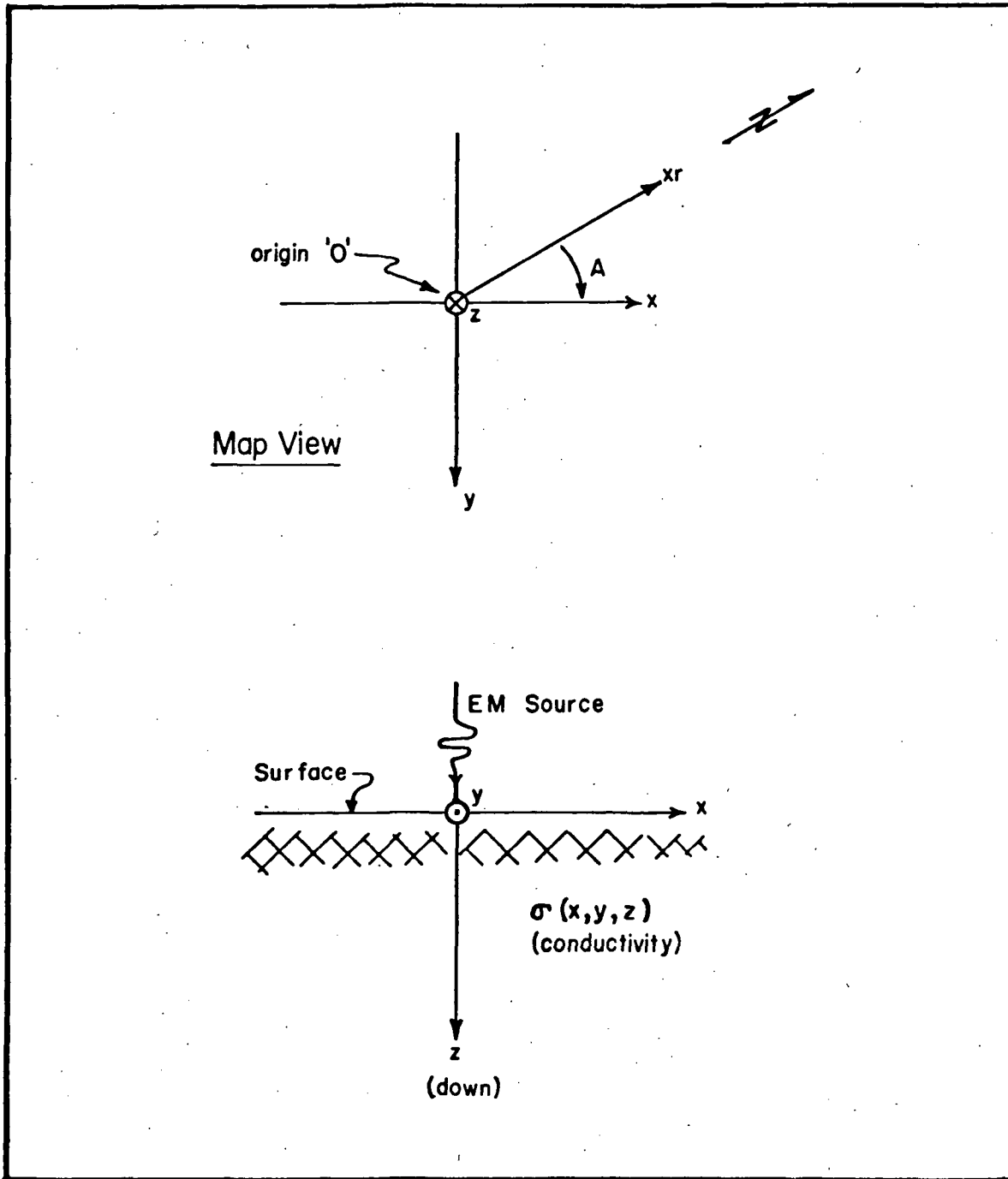


Fig. C-1: MT Co-ordinate System

PROPRIETARY INFORMATION NOTICE
 This document contains Geotronics Corporation proprietary and confidential information which is supplied for limited purposes only, and remains the property of Geotronics Corporation. This document may not be reproduced in whole or in part without written consent of Geotronics Corporation and the information therein must not be disclosed to persons not having need of such disclosure consistent with the License for which it is supplied. This document is to be returned to Geotronics Corporation upon termination of the License under which it is supplied.

Appendix D

MT Interpretation -- Defining Equations and Glossary of computed Quantities

(This appendix covers only the standard electrical interpretation process. See Appendix C for MT analysis information)

I. One-dimensional Inversion

The 1-D inversion process inputs ZTE(f) information (RTE and PTE are actually used) and produces a continuous resistivity-depth function, $R(z)$, that is an estimate of the smoothed true resistivity vs. depth under the measuring site. The algorithm used is an adaptation of a method devised by Dr. F. X. Bostick, Jr. at the University of Texas at Austin. The process, represented here by an operator 'B' is a forward going analytical approximation such that

$$R(z) = B \{ZTE(f)\} \quad (D-1)$$

The process produces two alternate models referred to as Amplitude Inversion (AI) and Phase Inversion (PI).

The AI version is used in the modeling and interpretation. The PI version, which has more inherent smoothing effect, is computed and used only for internal diagnostic purposes.

A pseudo depth-frequency correspondence, $z(f)$, is produced by the inversion process and can be used to relate other frequency domain functions to the depth scale in the model.

II. Anisotropy Factor and Anisotropy Sense

The anisotropy factor $AF(f)$ is defined by

$$AF(f) = RTM(f)/RTE(f) \quad (D-2)$$

and thus indicates the degree of separation between apparent resistivities parallel and normal to strike. $AF(f) = 1.0$ for a 1-D structure, and is in general non-unity if anisotropy or lateral inhomogeneity is present.

The anisotropy sense is derived from change in $AF(f)$ with frequency, or $AF'(f)$, which indicates whether an anomalous horizon is active at frequency f and whether it is apparently resistive or conductive. Because of the logarithmic depth nature of the MT response, the anisotropy sense is defined as the derivative in the log-log plane as

$$AS(f) = \frac{d(\log AF(f))}{d(\log f)} \quad (D-3)$$

The following rule applies to the structural horizon effective at frequency f :

$AS(f) = 0$, One-dimensional

$AS(f) > 0$, Resistive anomaly

$AS(f) < 0$, Conductive anomaly

where "anomaly" refers to a reflector that is laterally anomalous. AF and AS are related to the depth scale in the electrical model by the pseudo depth-frequency function $z(f)$.

III. Notes and Glossary of Terms

A. Notes

- 1) Other frequency domain quantities, including the Dip-axis azimuth and the 3-D indices, (See Appendix C) are also related to depth by the pseudo depth-frequency function $z(f)$ for interpretational use.
- 2) One-dimensional refers to variation in z -direction only, and variation in more than one direction is referred to as an "anomaly".
- 3) Units are MKS.

B. Glossary

- 1) $R(z)$ -- true resistivity vs. depth estimate (as a continuous function) from inversion of RTE (f), where AI mode is "amplitude inversion" and PI mode is "phase inversion".
- 2) $z(f)$ -- pseudo depth-frequency correspondence from RTE(f) to $R(z)$ inversion.
- 3) AF(f) -- anisotropy factor
- 4) AS(f) -- anisotropy sense
- 5) Dip-axis plots -- dip-axis angle (normally A(YZ)) data plotted on a log-polar scale in map view, with angle on the azimuth scale and depth (interpreted through the $z(f)$ function) on a log-radial scale.
- 6) Resistivity Section -- refers to a display of the true resistivity estimates ($R(z)$ data) contoured in a cross section format (horizontal or vertical).
- 7) Correlation Section -- refers to a display of the $R(z)$ curves superimposed at site locations in vertical cross

section format, with site-to-site correlations drawn between like features and signatures in the $R(z)$ curves. Interfaces or boundaries are assumed at the inflection points of the $R(z)$ curves.

Appendix E - Resolution

A precise statement of MT resolution and accuracy is not presently practical, if possible at all, for generally 3-D geometry. Error estimates must be in large part empirical and in some cases qualitative. This section discusses some probable upper bounds on the errors. It does not attempt to deal with all possible sources of error and does not set absolute bounds.

The smoothing effects that exist for the overall model are likewise difficult to define in precise analytical terms because a precise 3-D solution does not exist. The smoothing is essentially a volume averaging of the conductivity distribution. The computed resistivity for a given point in the model is the result of an averaging of the conductivity in some volume about that point in the actual structure. The dimensions of the averaging volume, which are roughly proportional to depth, are a complicated function of the structure; but to the first order, one can assume a spherical averaging volume with a radius of about 30 percent or more of depth. The computed resistivity function is the reciprocal of the smoothed conductivity function.

For approximately 1-D results and mild anisotropy (say less than 0.3 decade split in RTE and RTM), and for normal measurement noise, the model conductivity should be within about ± 10 to 20 percent of the actual smoothed conductive structure. This assumes no severe 3-D effects are present. The mean depths to the various resistive units or features shown by the resistivity-depth function should be normally within ± 10 to 20 percent of actual depths.

When a high degree of anisotropy is present a greater possible error can be assumed, although the RTE inverse is still normally a

CA - actual intrinsic conductivity

f - frequency

z - depth

SD - skin depth

- 1) For a particular depth z_1 in the model find the corresponding frequency f , from the pseudo $z(f)$ relationship mentioned in Appendix D.
- 2) Features near depth z_1 will be averaged if their dimensions are less than about $0.5 SD(f_1)$, where $SD(f_1)$ is the skin depth at frequency f_1 in one of the following resistivities:
 - a) the resistivity $R(z_1)$ if the resistivity of the feature in question is greater than $R(z_1)$
 - or b) the resistivity of the feature in question itself if it is less than $R(z_1)$
- 3) The model conductivity $C(z_1)$ is the average of $CA(z)dz$ over an interval of about $z_1 \pm 0.5 SD(f_1)$.

The above criteria can be used to assess the possibility of the presence of thin conductive or resistive zones not shown explicitly in a given region of the model.

Appendix F - Data Smoothing and Comments on Noise and Special Conditions

The 1-D continuous inversion operator requires as input an impedance versus frequency function, $ZTE(f)$, that is compatible with a 1-D geometry. The RTE and PTE curves must be continuous and behave as a minimum phase function such that the slope of RTE(f) in the log-log plane is $(PTE/45^\circ) - 1$ to a first order approximation. The phase is bounded by $0^\circ \leq PTE \leq 90^\circ$ and the slope of RTE in the log-log plane is bounded by ± 1 .

Results computed from the field data are smoothed using the above constraints to produce a continuous, minimum phase function for the 1-D inversion. The field data are recorded in the presence of generally 3-D structures and a certain amount of noise, and the smooth functions are extrapolated through frequency bands of evident 3-D effects or excessive noise, using both amplitude and phase information in the process. This method results in a minimum phase best fit to the data, but due to the 3-D effects and noise, the smoothing operation is to a certain degree an interpretive process.

The noise level was generally high throughout the survey area, and the data quality was below normal for most sites. Most of the noise was probably due to cultural activity, including power lines and roadways which were especially difficult to avoid in the narrow valley area. A reasonable interpretation of the MT response was feasible at most sites over the frequency range from about 0.003 to 50 Hz with varying degrees of confidence. One exception is site 9 where excessive noise rendered the low frequency RTE data unuseable.

A "non-minimum phase" property is found to occur in the low frequency data for some sites, in that the slope of RTE in the log-log

plane exceeds one and the phase exceeds 90° . Theoretical work recently performed by Geotronics indicates that the observed behavior strongly suggests an extremely conductive anomaly with an abrupt upper horizon and a very high resistive to conductive contrast (probably 100:1 or more). MT responses of this type have been occasionally observed only in areas of recent magmatic activity and are probably of special significance in the geothermal survey, suggesting a zone of extremely conductive (possible semi-molten) rock.

Table F-1 lists several status codes pertaining to the data for certain frequency ranges and corresponding depth ranges. The status codes pertain to noise conditions, 3-D effects, and non-minimum phase conditions, showing categories of possible uncertainty due to noise. The main purpose of these codes is to show a relative indication of confidence level and to call attention to special conditions such as areas of greater 3-D influence and non-minimum phase. The error limits pertain to the uncertainty in depth and resistivity of a given feature in the 1-D inverse $R(z)$ and should not be taken as precise bounds on the errors, which in most cases should tend toward the low end of the range.

SLN-132

TABLE F-1

X-Y PLOT DATA QUALITY

SITE	FREQUENCY RANGE	BELOW SITE DEPTH RANGE METERS	FEET	STATUS CODE
1	3. -.5 Whole Range	100-340	335-1110	2 (GAP) ‡
2	> .1 Whole Range	610	2000	2(GAP) ‡
3	TE: Whole Range TE > .1 TM4. -.1 Whole Range	665 125-665	2190 410-2190	1(Noise) 3(GAP) 2(GAP) ‡
4	TE > .2 TM 6. -.3 Whole Range	435 95-330	1425 310-1090	3(GAP) 1(Noise) ‡

Status Categories

- # 3-D effects (e. g. RTE/RTM decision erratic)
- * NMP (significant non-minimum phase)
- 0 error less than 20% on R & z, second order features are significant
- 1 error 20% to 50% on R & z, second order features are significant but with greater variance in R & Z
- 2 error 50% to 100% on R & Z, second order feature are not dependable
- 3 error over 50% possible, only first order features are significant
- 4 first order features are not dependable